

Reactive and Organosoluble Anatase Nanoparticles by a Surfactant-Free Nonhydrolytic Synthesis

A. Aboulaich, B. Boury, and P. H. Mutin*

Institut Charles Gerhardt Montpellier, UMR5253 CNRS-UM2-ENSCM-UM1, Université Montpellier 2- CC1701, Place Eugène Bataillon, 34095 Montpellier Cedex 5, France

Received April 28, 2010

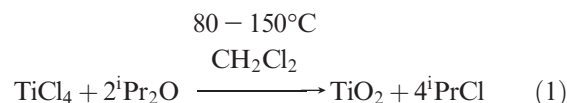
Revised Manuscript Received July 15, 2010

Last year, more than 10 000 publications were devoted to titanium dioxide (TiO₂), and among them, more than 500 dealt with nanoparticles and nanostructure aspects of this material. Owing to its unique properties, TiO₂ has attracted tremendous interest for environmental and energy applications,¹ including photocatalysis,² water-splitting³ and photovoltaic conversion.^{2,4} Accordingly, much effort has been devoted to finding new synthetic routes to TiO₂ nanoparticles. Since the first report by Colvin's group on the nonhydrolytic synthesis of titania anatase nanocrystals by reaction of titanium(IV) isopropoxide (Ti(OⁱPr)₄) with titanium(IV) chloride (TiCl₄) in the presence of trioctylphosphine oxide,⁵ nonhydrolytic (or nonaqueous) sol-gel routes⁶ have been found to provide particularly versatile and cost-effective methods for the synthesis of metal oxide nanoparticles with various structures, sizes and shapes. Several reviews have been recently dedicated to this topic.^{7–11} Nonhydrolytic routes have been found particularly useful to address several drawbacks of hydrolytic sol-gel, such as high and different hydrolysis-condensation rates of metal alkoxides, particle agglomeration and poor crystallinity of the crude precipitates.

Thus, TiO₂ nanoparticles have been prepared by different nonhydrolytic routes involving the reaction of titanium(IV) chloride or alkoxide precursors with various oxygen donors.^{11–14} In most cases, these syntheses were carried out in the presence of surfactants (e.g., trioctylphosphine

oxide, oleic acid or octylamine) in order to prevent the aggregation of the nanoparticles. These routes offer an excellent control over size and shape, but adsorbed surfactant may influence the toxicity of the nanoparticles and decrease both the accessibility to the nanoparticle surface and also its reactivity, which is a major drawback for applications in sensors or catalysis.^{15–17} In 2002, Niederberger et al. reported an elegant synthesis to TiO₂ nanoparticles in which benzyl alcohol is used as an oxygen donor, a solvent and a stabilizing agent.¹⁸ This “solvent-controlled” route was later extended to the synthesis of a large variety of metal oxide nanoparticles.¹¹

In this work we report the synthesis of TiO₂ anatase nanocrystals by reaction at 80–150 °C of TiCl₄ with a stoichiometric amount of diisopropyl ether (ⁱPr₂O) in dichloromethane (eq 1), *in the absence of surfactant or coordinating solvent*. This nonhydrolytic route (the so-called “ether route”) has recently proven successful for the preparation of mesoporous mixed oxide catalysts,^{19,20} and silica-based nanoparticles.²¹ We have previously reported the synthesis of TiO₂ powders by this route,^{22,23} but it has not been used so far to prepare titania nanoparticles. The novel results presented here show that heating dilute solutions of TiCl₄ and ⁱPr₂O in CH₂Cl₂ leads in high yields (> 80%) to phase-pure, unaggregated anatase nanoparticles, as sols or redispersible powders. In addition, the average size of the nanoparticles can be adjusted from about 4 to 15 nm depending on the reaction temperature. Interestingly, the surface of these nanoparticles present residual chloride and isopropoxide groups instead of hydroxyl groups. This unique surface chemistry accounts for the observed absence of aggregation and for the reactivity of the particles, for instance toward surface silanols or phosphonic acids, affording simple ways to form nanoparticles monolayers or to modify the surface of the particles with organic groups.



- (1) Chen, X.; Mao, S. S. *Chem. Rev.* **2007**, *107*, 2891–2959.
- (2) Thompson, T. L.; Yates, J. T. *J. Chem. Rev.* **2006**, *106*, 4428–4453.
- (3) Osterloh, F. E. *Chem. Mater.* **2008**, *20*, 35–54.
- (4) Burda, C.; Chen, X.; Narayanan, R.; El-Sayed, M. A. *Chem. Rev.* **2005**, *105*, 1025–1102.
- (5) Trentler, T. J.; Denler, T. E.; Bertone, J. F.; Agrawal, A.; Colvin, V. L. *J. Am. Chem. Soc.* **1999**, *121*, 1613–1614.
- (6) Mutin, P. H.; Vioux, A. *Chem. Mater.* **2009**, *21*, 582–596.
- (7) Jun, Y.-w.; Choi, J.-s.; Cheon, J. *Ang. Chem. Int. Ed.* **2006**, *45*, 3414–3439.
- (8) El-Sayed, M. A. *Acc. Chem. Res.* **2004**, *37*, 326–3363.
- (9) Park, J.-I.; Cheon, J. *J. Am. Chem. Soc.* **2001**, *123*, 5743–5746.
- (10) Steigerwald, M.; Brus, L. E. *Acc. Chem. Res.* **1990**, *23*, 183–188.
- (11) Pinna, N.; Niederberger, M. *Ang. Chem. Int. Ed.* **2008**, *47*, 5292–5304.
- (12) Koo, B.; Park, J.; Kim, Y.; Choi, S.-H.; Sung, Y.-E.; Hyeon, T. *J. Phys. Chem. B* **2006**, *110*, 24318–24323.
- (13) Jun, Y. W.; Casula, M. F.; Sim, J.-H.; Kim, S. Y.; Cheon, J.; Alivisatos, A. P. *J. Am. Chem. Soc.* **2003**, *125*, 15981–15985.
- (14) Seo, J.-W.; Jun, Y.-W.; Ko, S. J.; Cheon, J. *J. Phys. Chem. B* **2005**, *109*, 5389–5391.

- (15) Niederberger, M. *Acc. Chem. Res.* **2007**, *40*, 793–800.
- (16) Djerdj, I.; Arcon, D.; Jaglicic, Z.; Niederberger, M. *J. Solid State Chem.* **2008**, *181*, 1571–1581.
- (17) Niederberger, M.; Garnweitner, G. *Chem.—Eur. J.* **2006**, *12*, 7282–7302.
- (18) Niederberger, M.; Bartl, M. H.; Stucky, G. D. *Chem. Mater.* **2002**, *14*, 4364–4370.
- (19) Cojocariu, A. M.; Mutin, P. H.; Dumitriu, E.; Fajula, F.; Vioux, A.; Hulea, V. *Chem. Commun.* **2008**, *42*, 5357–5359.
- (20) Debecker, D. P.; Bouchmella, K.; Poleunis, C.; Eloy, P.; Bertrand, P.; Gaigneaux, E. M.; Mutin, P. H. *Chem. Mater.* **2009**, *21*, 2817–2824.
- (21) Aboulaich, A.; Lorret, O.; Boury, B.; H., M. P. *Chem. Mater.* **2009**, *21*, 2577–2579.
- (22) Arnal, P.; Corriu, R. J. P.; Leclercq, D.; Mutin, P. H.; Vioux, A. *J. Mater. Chem.* **1996**, *6*, 1925–1932.
- (23) Arnal, P.; Corriu, R. J. P.; Leclercq, D.; Mutin, P. H.; Vioux, A. *Chem. Mater.* **1997**, *9*, 694–698.

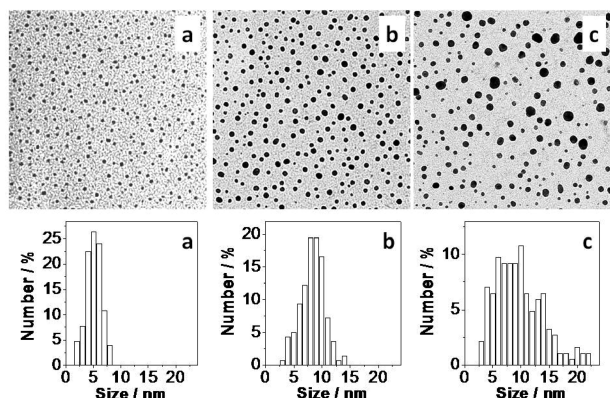


Figure 1. TEM images (400×400 nm) of nanoparticles of (a) $\text{TiO}_2,80$, (b) $\text{TiO}_2,110$, and (c) $\text{TiO}_2,150$ and corresponding size distributions.

In a typical synthesis, TiCl_4 and $i\text{Pr}_2\text{O}$ in CH_2Cl_2 were reacted in a sealed Pyrex tube for 60 h at 80°C , 110°C or 150°C (see Supporting Information). The sealed tube was then opened in a glovebox and the resulting white precipitates were centrifuged and washed with CH_2Cl_2 . The samples are denoted TiO_2X , where X is the reaction temperature ($^\circ\text{C}$). The yield of the syntheses (based on the weight of oxide after calcination of the precipitates) was excellent, $> 80\%$ in all cases.

The precipitates obtained after washing and gentle drying at room temperature could be redispersed in anhydrous THF even after several weeks of storage in inert atmosphere. Moisture or drying at high temperature must be avoided, as they may trigger condensation reactions leading to irreversible aggregation. TEM images of diluted sols deposited on a grid (Figure 1) revealed in all cases the presence of perfectly dispersed spherical nanoparticles. The size of the particles and also the width of the particle size distribution increased with the reaction temperature. The specific surface area of particles is given in Table 1. The value found for $\text{TiO}_2,80$ ($440 \text{ m}^2 \text{ g}^{-1}$) is among the highest reported for TiO_2 powders.^{18,24,25} The XRD patterns of the crude samples (Figure 2) exhibited reflections corresponding to anatase, no trace of rutile or brookite being detected. The crystallite sizes estimated from the broadening of the (101) reflection using the Debye–Scherrer’s equation were close to the particle sizes derived from the specific surface area calculation, confirming that the particles are nonporous anatase nanocrystals with sizes ranging from about 5 to 15 nm depending on the reaction temperature (Table 1).

The excellent dispersibility of the nanoparticles in organic medium is remarkable, particularly for a synthesis in the absence of surfactant or coordinating solvent, and allows to prepared solution of nanoparticles in THF (0.3% by weight). As previously reported for nonhydrolytic silica-based nanoparticles,²¹ this has to be related to the surface chemistry of the particles resulting from the reactions involved in the synthesis. Here, this implies

Table 1. Specific Surface Area of the Nanoparticles Deduced from Porosimetry Measurements and Sizes Estimated from the Specific Surface Area and XRD Patterns

Sample	S_{BET}^a ($\text{m}^2 \text{ g}^{-1}$)	D_{BET}^b (nm)	D_{XRD}^c (nm)
$\text{TiO}_2,80$	430	3.6	3.8
$\text{TiO}_2,110$	170	9.1	9.5
$\text{TiO}_2,150$	105	14.7	16.3

^a Specific surface area. ^b Particle size derived from the specific surface area, according to $D_{\text{BET}} = 6000/(\rho S_{\text{BET}})$ where ρ is the anatase density (3.9). ^c Crystallite size estimated from the broadening of the (101) reflection using the Debye–Scherrer’s equation.

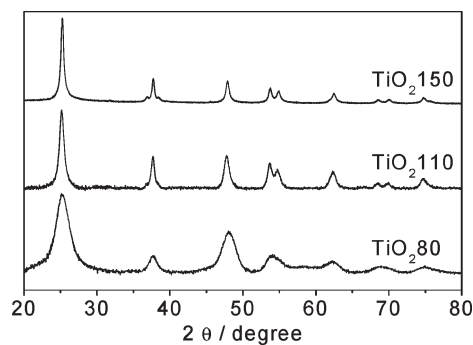


Figure 2. Powder XRD patterns of the nanoparticles.

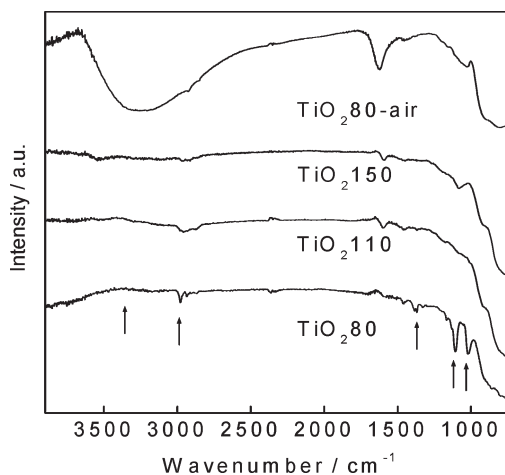
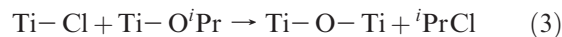
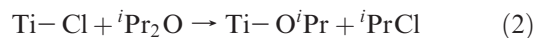


Figure 3. Transmission FTIR spectra of the nanoparticles of TiO_2 and of $\text{TiO}_2,80$ sample after exposure to ambient humidity for 30 min. The vibrations indicated by arrows are discussed in the text.

organophilic residual $\text{Ti}-\text{Cl}$ and $\text{Ti}-\text{O}^i\text{Pr}$ groups instead of hydrophilic $\text{Ti}-\text{OH}$ groups (eqs 2 and 3):



Indeed, the FTIR spectra of the nanoparticles (Figure 3) demonstrated the absence of hydroxyl groups (broad band between 3700 and 3200 cm^{-1}). In the case of $\text{TiO}_2,80$, vibrations at 1106 – 1010 , 1375 – 1385 cm^{-1} , and 2975 cm^{-1} ($\text{C}-\text{O}$, $\text{Ti}-\text{O}$, and CH_3 deformations and $\text{C}-\text{H}$ stretchings) indicate the presence of O^iPr groups.²⁶ These bands

(24) Niederberger, M.; Bartl, M. H.; Stucky, G. D. *J. Am. Chem. Soc.* **2002**, *124*, 13642–13643.

(25) Wang, C.-C.; Ying, J. Y. *Chem. Mater.* **1999**, *11*, 3113–3120.

(26) Moran, P. D.; Bowmaker, G. A.; Cooneykim, R. P.; Finnie, S.; Bartlett, J. R.; Woolfrey, J. L. *Inorg. Chem.* **1998**, *37*, 2741–2748.

Table 2. Composition and thermal analysis of the nanoparticles

sample	Ti–Cl ^a	C ^b	TGA weight loss ^c	average formula ^d
TiO ₂ 80	3.4	7.9	18.0	TiO _{1.72} (ⁱ Pr) _{0.22} Cl _{0.34}
TiO ₂ 110	2.2	4.7	14.0	TiO _{1.84} (ⁱ Pr) _{0.12} Cl _{0.20}
TiO ₂ 150	1.0	3.7	13.2	TiO _{1.91} (ⁱ Pr) _{0.09} Cl _{0.09}

^aHydrolyzable Ti–Cl content measured by acid–base titration (mmol g⁻¹). ^bC content measured by ICP-MS (wt%). ^cWeight loss (%) between 20 and 800 °C measured by thermogravimetric analysis in dry air flow (heating rate 10 °C min⁻¹) (%). ^dComposition derived from the Cl and C contents assuming the presence of Ti–Cl and Ti–OⁱPr groups.

are almost not detected on the samples prepared at higher temperature, possibly due to their lower surface area and/or to side reactions. The UV–vis spectra of the particles redispersed in THF (see Supporting Information) showed the expected strong absorption due to anatase below ca. 350 nm. In addition, the spectrum of TiO₂150 displays less intense bands in the visible region, which also suggests the occurrence at high temperature of side reactions leading to unsaturated organic compounds.

Exposure of the nanoparticles sols to ambient humidity leads after few hours to the irreversible formation of a soft gel. Similarly, exposure of the dried nanoparticles for 30 min lead to the evolution of HCl (confirming the presence of hydrolyzable Ti–Cl groups) and to the formation an insoluble solid. FTIR spectroscopy of the resulting solid showed the presence of hydroxyl groups (Figure 3) and to the disappearance of the bands related to OⁱPr groups. The amount of Ti–Cl groups (determined by acid–base titration), the carbon content of the nanoparticles and the weight losses found by thermogravimetric analysis (Table 2) demonstrate that the amount of residual groups increased with the surface area of the particles.

The presence of Ti–Cl and Ti–OⁱPr surface groups instead of hydroxyl groups makes the surface organophilic, and the negligible rate of nonhydrolytic condensation at room temperature prevents the aggregation of the particles (in the absence of water).

Furthermore, this surface chemistry and the absence of surfactant or bulky stabilizing groups make these TiO₂ nanoparticles very reactive. For instance, the ³¹P MAS NMR spectrum of TiO₂80 nanoparticles reacted with octadecylphosphonic acid (ODPA) in THF (see Supporting Information) showed a signal centered at 30 ppm, as expected for the surface modification of anatase with an alkylphosphonic acid.²⁷ This spectrum indicates that octadecylphosphonate groups are linked to the surface by Ti–O–P bonds, most likely resulting from the condensation of P–OH groups with surface Ti–Cl and T–OⁱPr groups.

The chloride and alkoxide groups at the surface of the particles can also condense with silanol groups allowing

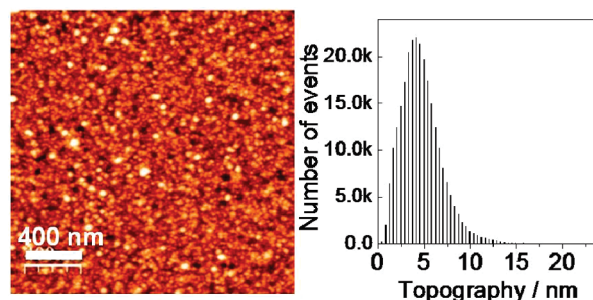


Figure 4. (a) AFM image of the surface of a silicon wafer after dipping for 2 h in a TiO₂80 sol in THF and (b) corresponding height distribution.

the grafting of the nanoparticles at the surface of an hydroxylated substrate. Thus, the AFM image of an oxidized silicon wafer immersed in a sol of TiO₂80 nanoparticles in THF (0.3 wt % TiO₂) for 2 h at 25 °C reveals that a single monolayer of nanoparticles was irreversibly grafted onto the wafer surface (Figure 4).

The self-limiting aspect of this grafting can be ascribed to the absence of Ti–Cl/Ti–OⁱPr condensation (at room temperature and in the absence of water) which prevents the formation of multilayers by reaction of nanoparticles with the first layer. Finally, the resulting TiO₂ coating can be further modified with ODPAs, leading to an hydrophobic surface with a water contact angle of $\Theta = 102^\circ$.

As a conclusion, the results reported here demonstrate that the reaction of TiCl₄ with a stoichiometric amount of ⁱPr₂O in the absence of surfactant or coordinating solvent offers a convenient route to single-phase anatase nanoparticles. The average size of the nanoparticles can be easily adjusted between about 4 to 15 nm by playing on the reaction temperature. The nanoparticles are not hydroxylated but appear covered with TiOⁱPr and/or TiCl groups. This surface chemistry accounts for three important points: the lack of aggregation, their dispersibility in organic medium, and their reactivity toward water, phosphonic acids, or silanol groups. The absence of nonhydrolytic condensation at room temperature prevents the aggregation of the particles and allows the self-limiting grafting of nanoparticle monolayers. The excellent yield and the simplicity of the synthesis, which can be easily scaled to prepare multigram quantities of TiO₂ nanoparticles, is also worth noticing.

Acknowledgment. The Centre National de la Recherche Scientifique and the Ministère de l'Enseignement Supérieur et de la Recherche are gratefully thanked for supporting this work.

Supporting Information Available: Experimental part, TGA analysis of the nanoparticles, UV–vis spectra of the particles in solution, and ³¹P MAS NMR spectrum of TiO₂80 reacted with ODPAs (PDF). This information is available free of charge via the Internet at <http://pubs.acs.org/>.

(27) Brodard-Severac, F.; Guerrero, G.; Maquet, J.; Florian, P.; Gervais, C.; Mutin, P. H. *Chem. Mater.* **2008**, *20*, 5191–5196.